Flood Hazard, Vulnerability and Risk Assessments for Uttarakhand State in India

Varsha Hassan Vishwanath
Center for Geographic Information Science and Technology (CGIST)
Rochester Institute of Technology
vh6928@rit.edu

Brian Tomaszewski
Center for Geographic Information Science and Technology (CGIST)
Rochester Institute of Technology
bmtski@rit.edu

ABSTRACT

The Indian state of Uttarakhand, located in the valleys of the Himalayan Mountains, is severely prone to flash floods. High intense rainfall, river channels and slope are some of the significant factors responsible for flash floods. In this work-in-progress paper, we addressed these challenges via flood risk analysis in a geoprocessing framework that utilized hazard and vulnerability assessments, computed using hydrologic and demographic data by employing Analytical Hierarchy Process (AHP). The resulting maps indicated that flood risk regions have significant correspondence with regions that are highly hazardous and vulnerable. These maps could help develop better disaster management measures for Uttarakhand. Flash floods still being a globally challenging problem, these methods could be used to expand research to improve flash flood predictions and warning systems in many countries.

Keywords

Flood risk, DEM, GIS, India, Uttarakhand.

INTRODUCTION

Floods are the most catastrophic and the most frequently occurring natural disaster across the world. Floods are responsible for 47% of all weather-related disasters (UNISDR, 2015). About 6.8 million people died of floods in the 20th century. Statistically, 2.8 billion people have been affected (Doocy S, et al., 2013) with an average of more than 80 million affected each year across the globe in the last 30 years (Bhatt, et al., 2014). The repercussions include 4.5 million homeless, 540,000 deaths, 360,000 injuries and millions unrecorded (Doocy, et al., 2013). Economic loss for the last thirty years amounts to more than $11 billion. Between 1994 and 2004, Asia has seen approximately 1,500 flood disasters (Bhatt, et al., 2014).

The Indian sub-continent is highly vulnerable to natural disasters like floods, earthquakes and landslides. The state of Uttarakhand, which is located at the foothills of Himalayas, with China and Nepal as its neighboring countries (see Figure 1), is severely prone to floods and flash floods. Furthermore, flash floods often trigger landslides, and mudslides in regions that are geologically unstable. Some of the major events that have occurred in the last 30 years are Malpa flood and landslide of 1998 in Pithiragarh, Rudraprayag flood in 2001, Tehri flood of 2002 and Varunavat flood of 2003 (Pande, 2010).

In June 2013, people of Uttarakhand witnessed one of the worst flash floods seen in over a century. More than 6,000 people died, which is the highest for that year (Wake, Bronwyn, 2013), and thousands more were affected (Cho, et al., 2016). According to the Indian Meteorological Department (IMD), most regions received between 300mm and 400mm of rainfall within a span of four days, 14 – 18 June 2013. This torrential rain, caused by a cloudburst, ravaged the state that had already been subjected to high intense rainfall a few days before, 10 -11 June 2013, which had completely saturated the soil (Rao, et al., 2014; Martha, et al., 2015). The significant run-off that soon ensued was not only because of pre-saturated soil, but also from rapid snowmelt (Cho, et al., 2016).

Figure 1. Geographic Map of the Study Area

Consequently, the cumulative effect was two catastrophic flash flood events that led to land and mudslides, Mandakini river flooding, channel shifts, Lake Chorabari breach, destroying multiple settlements and thousands of lives. Kedarnath settlement, located along the banks of river Mandakini and a few hundred meters below Lake Chorabari, was completely wiped out by the disaster (Dobhal, et al., 2013, Rao, et al., 2014). The panchromatic satellite images of the settlement before and after the flash floods are shown in figure 2.

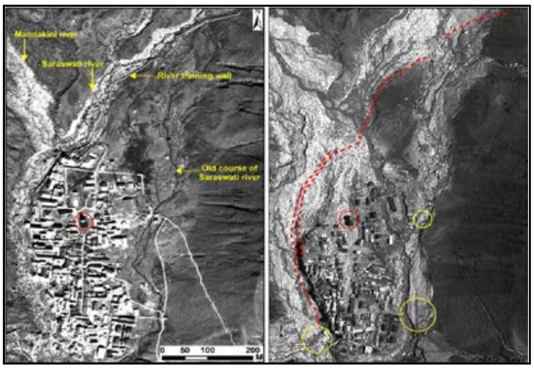

Figure 2. Left image is the pre-disaster 2.5 m resolution panchromatic image from GeoEye, and the right image is the post-disaster 2.5 m resolution CARTOSAT panchromatic image (Martha et al., 2015)

Even though, we have made significant advances in flood forecasting and early warning systems, flash floods are still a challenge because they occur due to intense short bursts of rainfall and measuring the intensity and duration of high intense rainfall is extremely difficult (National Research council, 2005; Rao, et al., 2014). Flash floods mostly occur in complex mountainous regions (National Research Council, 2005). Historically, heavy rainfall and cloudburst have been the main factors for floods in this region. (Bhambri, et al., 2016). High elevations, dense river network and the soil type have augmented the severity of flash floods. (Danumah, 2016; Hill, Firoz, 2010). Furthermore, state-wide hydro-electric power plants have been claimed to have intensified the impacts of floods (Sati and Gahalaut, 2013). This is because, these projects involve deforestation, blasting and tunneling and constructions in regions without proper inspection of the layout. Projects without proper inspection are geologically hazardous, as a significant portion of the state is situated on highly active seismic plates and disturbances could trigger floods and landslides (Ray, et al., 2016; Martha, et al., 2015; Sati and Gahalaut, 2013). Lack of significant information regarding the topographical and meteorological factors, rugged terrain and dense vegetation are major obstacles for having better disaster management relief.

June 2013 flash floods drew the attention of the scientific community, and an increasing number of research has been carried out ever since. Rao, 2014 carried out a comprehensive hydrological and hydraulic simulation study for Kedarnath town that quantified the causes of the flash floods. An extensive study about the devastation in terms of property damage for the regions of Garhwal and Kedarnath was carried out by Bhambri, et al., 2016. Number of landslides triggered by the flash floods were studied by Martha, et al., 2015. Cho, et al., 2016 took a different approach and carried out a comprehensive research on anthropogenic causes for climate change that caused the flash floods using Coupled Model Intercomparison Project Phase 5. Despite the wide variety of research, there are not many studies performed regarding flood risk management. Although, Bhatt, et al., 2014 carried out flood hazard and risk assessment for Chamoli district, a thorough research for flood risk analysis for the whole state is yet to be performed.

Multi-Criteria Analysis (MCA) has been popularly used by many researchers across the world to carry out flood risk analysis. Danumah, et al., 2016 used MCA to perform flood hazard and risk analysis for Abidjan district in Cote d'Ivoire. MCA was used for studying the flood hazard zones in Rhodope-Evros region in Greece by

Kazakis, et al., 2015. Matori, et al., 2014 used MCA methodology to identify flood prone zones in Perlis, Malayesia. Most of the research is limited either to a small region and /or for hazard or risk analysis. There are not many works on flood hazard, vulnerability and risk analyses for a whole state, which is data demanding and complicated. This is the issue addressed in this research.

This paper describes an extensive investigation of a variety of topographical and hydrological factors responsible for flash flood events in Uttarakhand state that are then applied to a geoprocessing framework using MCA. A series of maps were generated based on each factor, which were used to create hazard, vulnerability and risk index maps for the entire state. These maps provide a wealth of information that could prove to be useful across departments and organizations that are collectively responsible for decision making processes during flood disasters. The rest of the paper is divided into the following sections – study area, data sets, methods, results, discussions, summary, conclusion and future work.

STUDY AREA

Uttarakhand is a state in the Northern part of India, which shares international border with Tibet in the North and Nepal in the East. To the South and the West are two Indian states, Uttar Pradesh and Himachal Pradesh respectively, as shown in figure 1. The geographic extent of the state is 31.469° N, 79.062° E in the North, 30.25° N, 81.02° E in the East, 29.56° N, 77.99° E in the South and 31.06° N, 77.806° E in the West, with a total area of 20,650 sq. miles. The diverse topography includes glaciers, large number of perennial rivers, rugged mountainous terrain and dense forests. The elevation of the region varies greatly between 300 and 8,000 meters. About 68.4% of the state is covered by evergreen forests and 85% by mountains (Bhambri, et al., 2016; Bhatt, et al., 2014; Shresthta and Zinck, 2001). The topographical map is shown in figure 3.

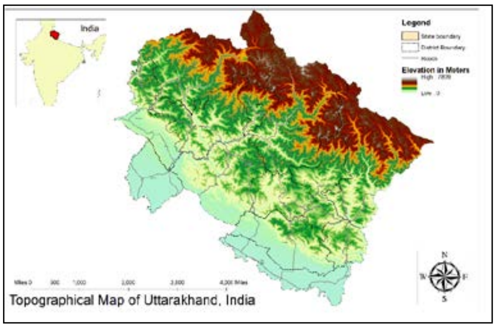

Figure 3. Topographic map of Uttarakhand state depicting elevation range from 0 to 7,809 m, river network, highways, state and district boundaries. An inset of a map of India shows the geographical location of the state.

DATA SETS

Conceptually, hazard, related to flood events, is characterized by the law of probability that considers factors related to natural phenomena, like hydrological and meteorological, and anthropogenic activities for a region. Vulnerability determines the damage sustained by the socioeconomic factors like demography for the region due to the disaster caused by the above factors. Risk, for a region, is determined as a product of hazard and vulnerability (Gilard,2016). Therefore, to compute flood risk, flood hazard and vulnerability assessments must be first carried out. The datasets used for hazard and vulnerability assessments are described below:

For hazard assessment precipitation, drainage density, soil moisture and slope datasets were used. Tropical Rainfall Measuring Mission (TRMM) precipitation raster dataset from 1998 – 2013 was obtained from NASA's Giovanni website. (Acker and Leptoukh, 2007). Shuttle Radar Topography Mission (SRTM) 30 m resolution Digital Elevation Model (DEM) data was obtained from USGS's EarthData website (NASA LP DAAC, 2000; Kobrick and Crippen). A total of 16 DEM raster tiles were obtained to cover the entire study area. Soil Moisture Index (SMI) data from National Oceanic and Atmospheric Administration's (NOAA) Earth System Research Laboratory (ESRL) (Dool, et al., 2003). Hydrography (river network) was obtained from MapCruzin website (MapCruzin). Population, settlements, places and road network vector datasets required for vulnerability assessment were all obtained from MapCruzin (MapCruzin).

METHOD

There are a lot of methods for flood risk analysis – quantitative, semi-quantitative and qualitative like indicator-based approach – of which quantitative is the more comprehensive method that not only identifies the potentially flood-risk areas, but also helps in cost benefit analysis, important for recovery stage. The method involves quantifying all the components considering a variety of aspects of flood events – temporal probability of hazards with intensity and frequency, spatial probability of vulnerabilities and intensity of exposure at risk elements. The downside of such quantitative methods is that they are data demanding and difficult to apply for larger study area and/or regions that sufficiently lack data (Van Westen, 2016). Event-tree approach, a semi-quantitative method is used for flood risk analysis, which mainly focuses on multi-hazard or multi-disaster events and their frequency, which is not the focus of this research. For a large region like Uttarakhand, that is challenged by its terrain, remoteness, and lack of sufficient data, a more qualitative approach is appropriate, like the indicator-based approach. This method utilizes the indicators of hazard and vulnerabilities to assess the risk of the study area (Van Westen, 2016). Multi-Criteria analysis is a popular indicator-based approach that is used to carry out a holistic assessment of the indicators or variables to compute risk analysis by using remotely sensed data where quantitative ground data is lacking. The MCA method and algorithm used in this research is explained in detail in the following paragraphs.

Multi-Criteria Analysis (MCA) is a decision-making method for solving complex problems that involve multiple variables, high degree of uncertainty, many alternatives and scientific and socioeconomic challenges. Analytical Hierarchy Process (AHP) is the algorithm used as a part of MCA for hazard and vulnerability assessments. The entire analysis is carried out in a geoprocessing workflow using ArcGIS. The steps taken are describes as follows:

1. Set the final goal for the problem - Flood Risk Index Map is the final goal.
2. Consider the factors influencing the problem and collect data accordingly - Hydrologic, topographic and demographic factors.
3. Divide the problem into different levels - Level 1: Variables – Datasets. Level 2: Criteria – Hazard and vulnerability assessments. Level 3: Goal – Flood Risk Map
4. Solve each criterion using AHP.
5. Combine the intermediate results (from level 2) to obtain the final goal.

Data Preparation

The entire data preprocessing workflow for hazard and vulnerability assessments are presented below in the figures 4 and 5.

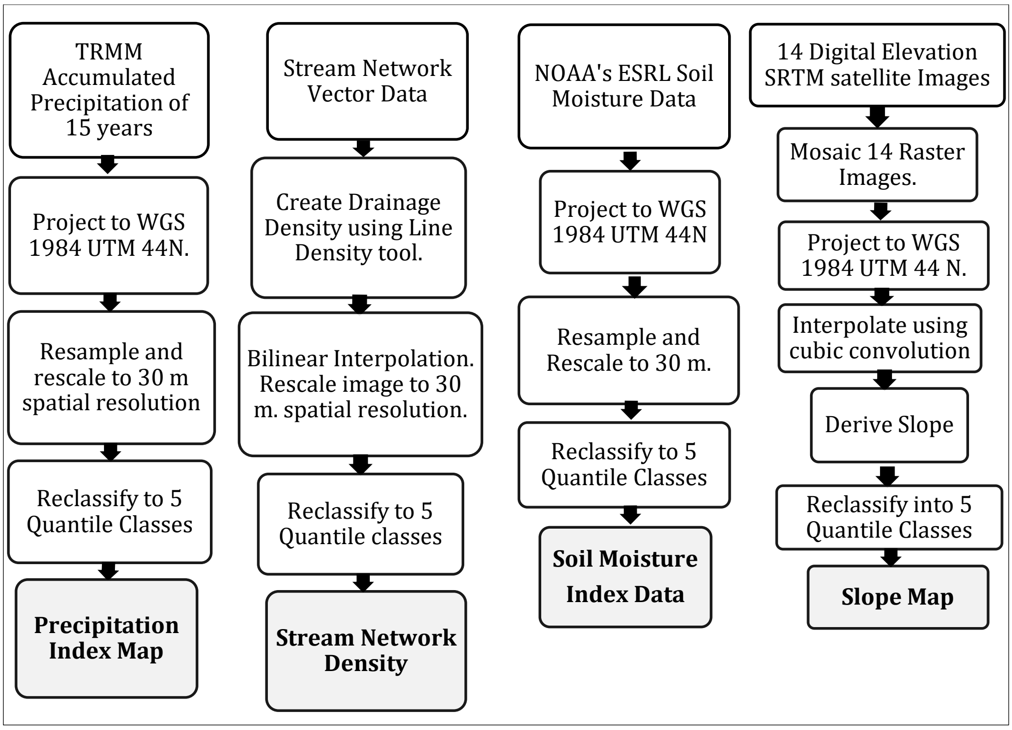

Figure 4. Data Preprocessing Workflow for creating Variables to be used in AHP for Hazard Assessment

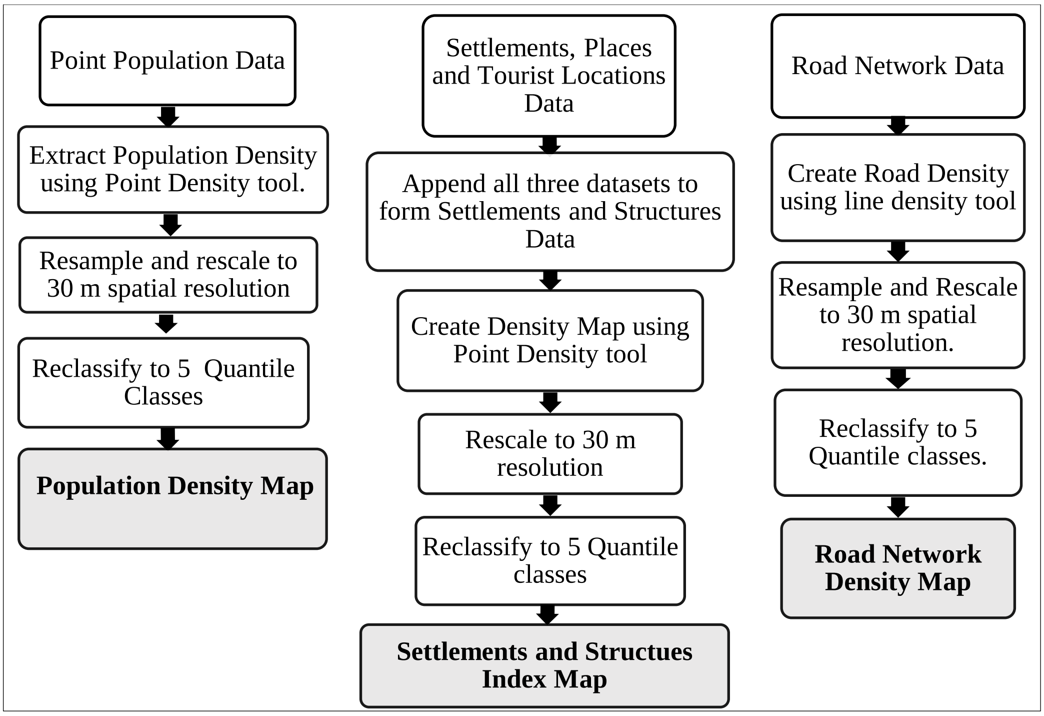

Figure 5. Data Preprocessing Workflow for creating Variables to be used in AHP for Vulnerability Assessment

Analytical Hierarchy Process (AHP):

AHP is most widely used for solving complex problems in which pairwise comparison is carried out between two variables by assigning weights according to Saaty scale, which is explained in table 1 (Danumah, et al., 2016; Kazakis, et al., 2015, Saaty, 1980).

Table 1. Saaty Scale used in AHP

Weights	Priority of the weights	Description
1	Equally Important	When both variables are equally significant to the criteria.
3	Slightly Important	One variable is mildly significant than the other.
5	Moderately Important	One variable is moderately significant than the other.
7	Strongly Important	One variable has higher significance than the other
9	Extremely Important	The variable has the highest significance to the objective.
2, 4, 6, 8	Intermediate preference between the weights	When compromise is needed between the two variables.

In AHP table, the variables are listed as attributes of comparison in the same order as row and column headers. Each row variable is compared with each column variable and input weights are assigned from the Saaty table based on the priority of the row variable. For instance, a value of 1 is entered as input if either a variable is compared with itself or the two variables have equal importance. When a value is entered for a row variable, then the reciprocal of the weight is assigned to the corresponding column variable that is listed along the row. The AHP tables for hazard and vulnerability assessments are shown in tables 2 and 3, which consist of input weights from the Saaty table, their normalized values (designated by their variable names with Nr as subscript), Priority Vector (PV) and Weighted Sum (WS). Weighted Sum is calculated by creating a matrix of elements obtained by each column of the input weights with corresponding priority weights. Then, the sum of each row gives the Weighted Sum (WS) for the matrix. To get consistent results, Consistency Ratio (CR) must be less than 0.1, which is calculated using Consistency Index (CI), Random Index (RI) and maximum eigenvalue (λ_{max}). Random Index (RI) (see Table 4) is selected from the Random Index Table based on the number of variables (Danumah, et al., 2016; Kazakis, et al., 2015; Saaty, 1980). The input weights for the AHP are based on extensive literature review, which is explained in detail after the AHP tables and calculations.

Table 2. Flood Hazard Assessment AHP Table.

Variables	PRP	DD	SOIL	SLP	PRP_{Nr}	DD_{Nr}	$SOIL_{Nr}$	SLP_{Nr}	PV	WS
PRP	1	3	5	7	0.5966	0.6618	0.5357	0.4375	0.5579	2.3541
DD	0.333	1	3	5	0.1986	0.2206	0.3214	0.3125	0.2632	1.0983
SOIL	0.2	0.333	1	3	0.1193	0.0734	0.1071	0.1875	0.1218	0.49142
SLP	0.143	0.2	0.333	1	0.0853	0.0441	0.0356	0.0625	0.0568	0.22971
Total	1.676	4.533	9.333	16						

PRP = Precipitation, DD = Drainage Density, SLP = Slope

$$\lambda_{maxH} = Average\left(\frac{WS}{PV}\right) \quad (1)$$

Where, λ_{maxH} is the maximum eigenvalue for hazard variables.

$$\lambda_{maxH} = \left(\frac{2.3541}{0.5579} + \frac{1.0983}{0.2632} + \frac{0.49142}{0.1218} + \frac{0.22971}{0.0568}\right)/4$$

$$\lambda_{maxH} = 4.1177 \quad (2)$$

$$CI = \frac{\lambda_{maxH} - n}{n-1} \quad (3)$$

$$CI = 0.0392 \quad (4)$$

$$CR = \frac{CI}{RI} \quad (5)$$

$$CR = 0.043 \quad (6)$$

In equation (5), RI = 0.9 for 4 variables (See Table 4).

Table 3. Flood Vulnerability Assessment AHP Table.

Variables	POP	SS	RD	POP_{Nr}	SS_{Nr}	RD_{Nr}	PV	WS
POP	1	3	5	0.6523	0.6923	0.5555	0.6333	1.945
SS	0.333	1	3	0.2172	0.2307	0.3333	0.2604	0.78958
RD	0.2	0.333	1	0.1304	0.0768	0.1111	0.1061	0.31946
Total	1.533	4.333	9					

POP = Population, SS = Settlements and Structures and RD = Road.

$$\lambda_{maxV} = Average\left(\frac{WS}{PV}\right) \quad (7)$$

Where, λ_{maxV} is the maximum eigenvalue for vulnerability variables.

$$\lambda_{maxV} = \left(\frac{1.945}{0.6333} + \frac{0.78958}{0.2604} + \frac{0.31946}{0.1061}\right)/3$$

$$\lambda_{maxV} = 3.0381 \quad (8)$$

$$CI = \frac{\lambda_{maxV} - n}{n-1} \quad (9)$$

$$CI = 0.01905 \quad (10)$$

$$CR = \frac{CI}{RI} \quad (11)$$

$$CR = 0.032 \quad (12)$$

In equation (11), RI = 0.58 for 3 variables (See Table 4).

Table 4. Random Index Table

Number of Variables	RI
2	0.00
3	0.58
4	0.9
5	1.12
6	1.24
7	1.32
8	1.41
9	1.45
10	1.49

Flash floods mostly occurs in complex terrain by orographic precipitation, which occurs by the influence of mountains or sometimes by hurricanes and tropical systems (Azmeri, et al., 2016; Hill and Firoz, 2010; Nation Research Council, 2005). Most flash floods are mainly triggered by high intense rainfall. However, there are other hydrological factors that also contribute to the cause. River channels, terrain slope, soil type and moisture, vegetation, landuse, snow melt and lake breach are some of them (Azmiri, etal., 2016; Bhambri, et al., 2016, Hill and Firoz, 2010; Martha, et al., 2015, National Research Council, 2005; Ray, et al., 2016). Azmeri, et al, 2016, Bonacci, O., et al, 2006, Kazakis, et al, 2015, Matori, et al, 2014, Strudevant-Rees, et al., 2001 have all considered intense rainfall as the main cause for floods in their research. Cloudburst and high intense rainfall were also the main causes for flash floods in Uttarakhand (Bhambri, et al., 2016; Cho, et al., 2016; Rao, et al., 2014; Sati and Gahalaut, 2013). Therefore, precipitation was given a higher weight in comparison to drainage density, soil and slope in the AHP table.

Large number of river channels near settlements is hazardous because greater drainage density causes channels to overwhelm with additional run-offs, thereby flooding the region (Hill and Firoz, 2010). Kedarnath is the perfect example for this situation, as it is situated on the banks of river Mandakini, which completely devastated the town (Bhambri, et al., 2016; Martha, et al., Rao, et al., 2014). Danumah, et al., 2016 and Kazakis, et al., 2015 considered drainage density as second hazardous factor in their research as well. For the number of perennial rivers that flow close to the settlements, and the close hydrological connection between intense rainfall and river flooding, drainage density was a more hazardous factor compared to slope and soil.

Soil moisture index is crucial for the run-offs. During monsoon seasons, due to normal antecedent rains soil gets saturated, which leads to increasing run-offs during intense rainfall. However, it was considered relatively less crucial compared to the former factors for causing flood hazards because it relatively less hazardous if there are no pre-saturation conditions.

Slope influences the run-off factor during intense rainfall. Steeper terrain causes lesser water to be absorbed leading to significant run-offs both ono surface and in channels. However, it is more hazardous when steepness is low as water floods in low elevated regions (Kazakis, et al., 2015). Since most of Uttarakhand has higher elevations slope was assigned the least weight in pair-wise comparison in AHP.

Finally, flood risk map is generated as product of flood hazard and vulnerability assessment results. The entire workflow is shown in figure 6, which represents all three levels – variables, criteria and goal.

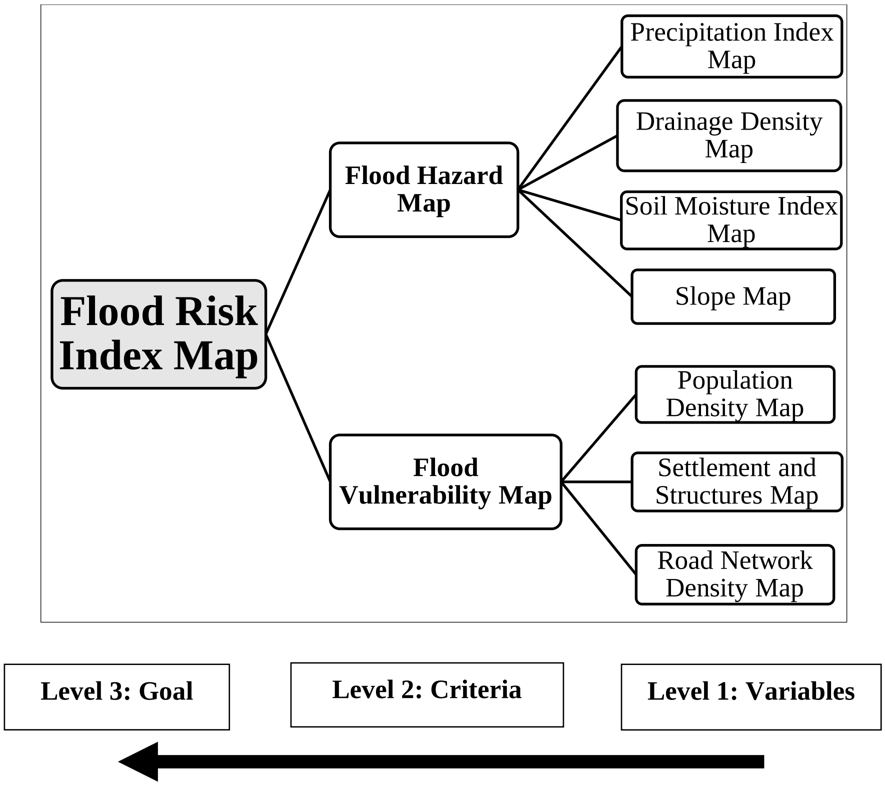

Figure 6. Multi-Criteria Analysis Workflow for Flood Risk Analysis

RESULTS

A total of 13 maps were generated from all the workflows in ArcGIS and were classified in 5 classes that are tabulated below:

Table 5. Map Classes

Index	Class	Color
1	Very Low	Dark Green
2	Low	Green
3	Medium	Yellow
4	High	Orange
5	Very High	Red

The results of preprocessing workflow for hazard assessment are thematic maps of precipitation, drainage density, soil moisture and slope. These are displayed in figures 7 and 8. Figure 9 is the Flood Hazard Map which was obtained by using the above maps as input variables to AHP hazard assessment table.

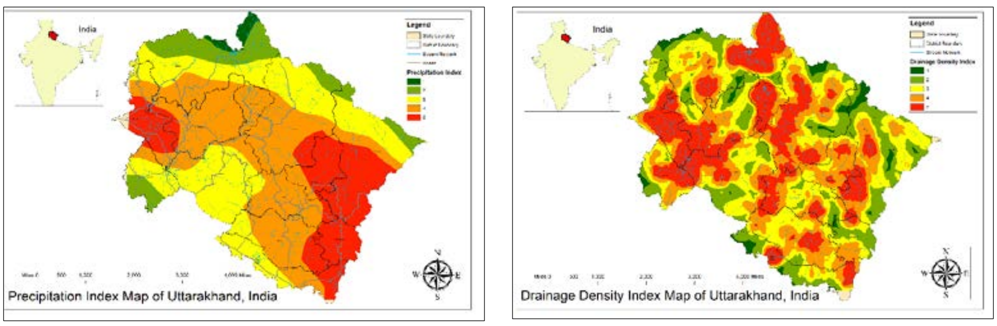

Figure 7. Precipitation and Drainage Density maps obtained from flood hazard preprocessing steps

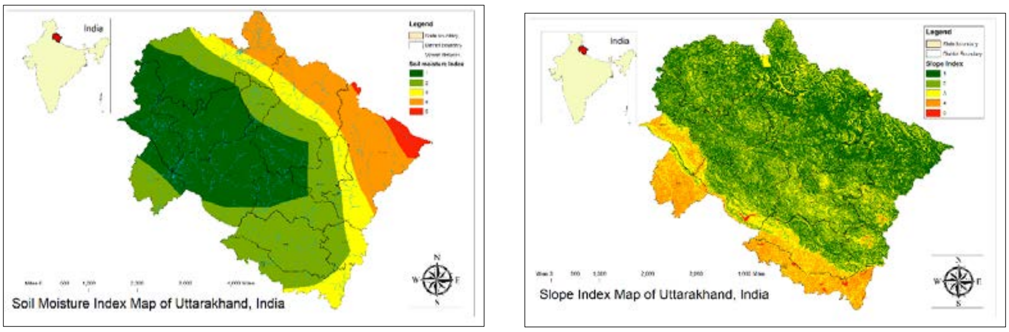

Figure 8. Soil Moisture and Slope Maps of Uttarakhand State, India

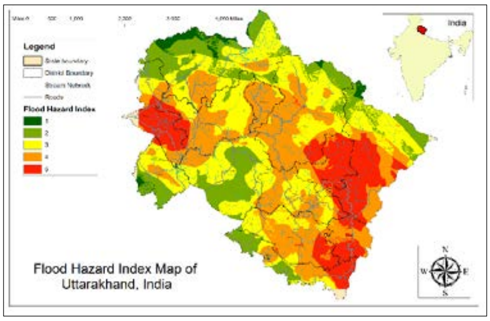

Figure 9. Flood Hazard Index Map. Classes 4 and 5 hazard regions correspond with that of Precipitation and Drainage Density regions

Data preprocessing results for vulnerability assessment were population density, settlements and structures, and road density maps. These are displayed in figure 10. Using these as inputs to vulnerability AHP table, flood vulnerability index map was created that is shown in figure 11.

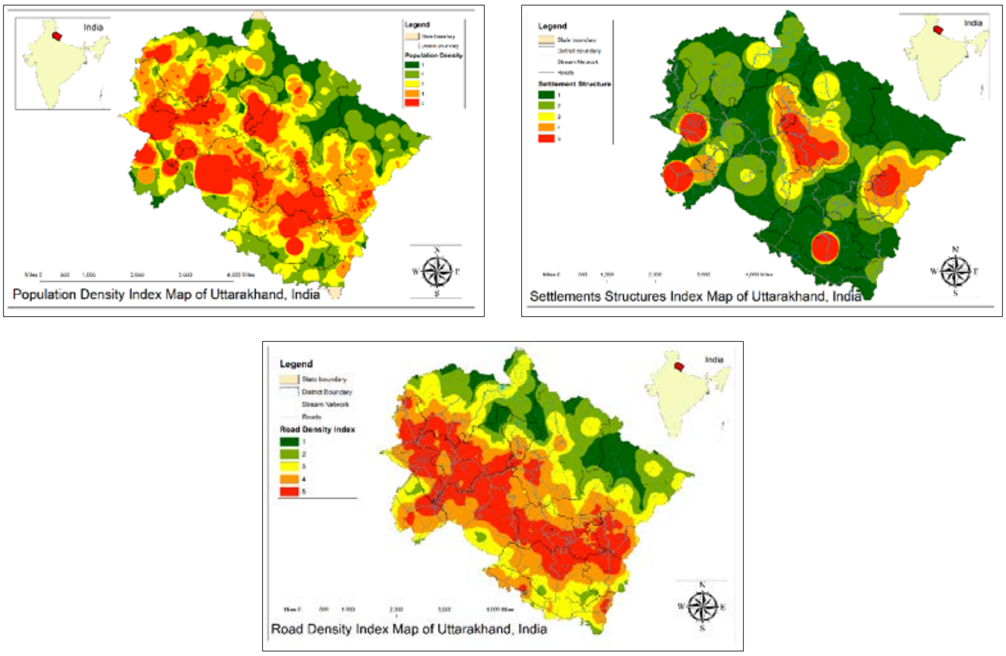

Figure 10. From top left clockwise: Maps of Population Density, Settlements and Structures, and Road Density

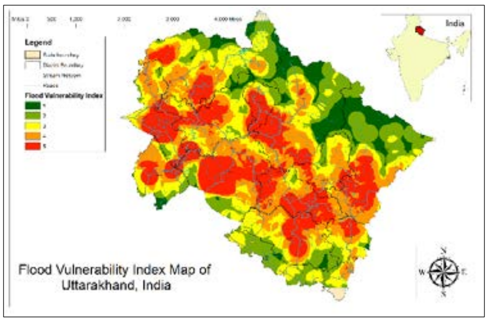

Figure 11. Flood Vulnerability Index Map. Evidently, highly vulnerable regions correspond with areas of high population density and settlements and even road network despite assigning lower weights.

The product of flood hazard index and vulnerability index maps is the flood risk map that is shown in figure 12. Figure 13 shows two overlay maps of flood risk – one with major hydro power plant locations and the other with locations of historical flood events that evaluates the results of the analysis.

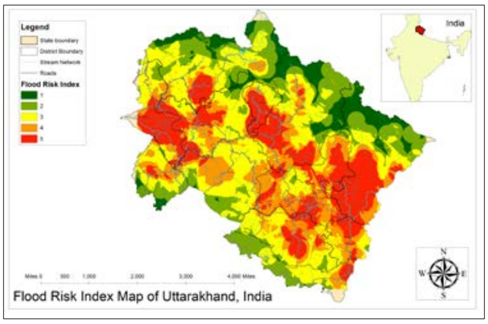

Figure 12. Flood Risk Index Map of Uttarakhand

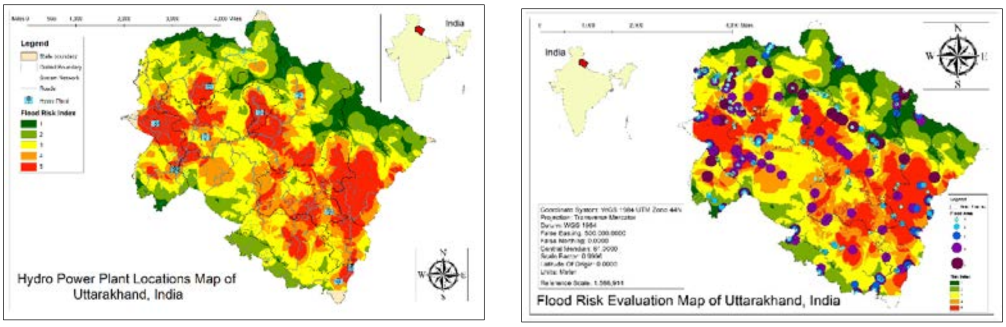

Figure 13. On the Left is a map of Flood Risk overlaid with Hydro Power Plant Locations, many of which are in high risk zones. On the Right is Flood Risk Map overlaied with locations of historical flood events. These events are represented by graduated dot density. So the large purple dots represent greater number of flood events that mostly coincide with classes 4 and 5 of the risk index.

Analytical results of multi-criteria analysis using AHP for flood hazard and vulnerability assessments in geoprocessing framework using ArcGIS are tabulated below.

Table 5. Flood Hazard Assessment Analytical Results. CR = 0.043

Variables	Eigenvalues	Eigenvectors	Criteria Weights
Precipitation	4.117	0.888	56.5009
Drainage Density	-0.0037	0.4121	26.2201
Soil	-0.0037	0.1847	11.7504
Slope	-0.1095	0.0869	5.5285

Table 6. Flood Vulnerability Assessment Analytical Results. CR = 0.036

Variables	Eigenvalues	Eigenvectors	Criteria Weights
Population	3.0385	0.9161	63.6986
Land Use	-0.0193	0.3715	25.8285
Road	-0.0193	0.1506	10.4729

DISCUSSION

Variable Classification

The classification of each variable is based on the degree of influence a variable has on hazard or vulnerability and the type of relation it has with the index factor: direct or inverse. For instance, precipitation has a direct relation with the index factor. Lower precipitation regions are assigned classes 1 and 2, while higher precipitation regions are classified 4 and 5 indicating that they are highly prone to flood hazards. Similarly, low population density regions are classified as 1 and 2 because they are less vulnerable to flood disasters, whereas high population density regions are assigned classes 4 and 5 as they are more vulnerable.

Soil moisture index and slope are the only two variables that are inversely related to the index factor. Soil moisture data obtained from NOAA's ESR Laboratory is created using water heights in soil (Dool, et al., 2003). Therefore, regions with low moisture index have low water heights indicating lesser moisture absorption capability and therefore are more prone to flood hazards. However, regions with high soil moisture index have better moisture absorption capability and are therefore less susceptible to flood events. Hence, in the reclassification step, low soil moisture regions were assigned classes 4 and 5, and high soil moisture regions were classified as 1 and 2.

Extending the same concept to slope, regions with higher steepness or slope are assigned classes 1 and 2, and regions with low slope are classified as 4 and 5. This is because, during heavy rainfall, water flows down quickly in steeper regions, which decreases stagnation. On the other hand, in less steep regions, water flows slowly, which overwhelms the river channels and cause flooding. Therefore, flat lands are more prone to flood hazard than steeper regions (Danumah, et al., 2016, Kazakis, et al.,2015).

Flood Hazard Assessments:

According to the analytical results of hazard assessment shown in table 4, 56.5% of the flood hazard is caused by precipitation and 26.2% by drainage density. This result is consistent with the studies Azmiri, etal., 2016; Bhambri, et al., 2016, Hill and Firoz, 2010; Martha, et al., Rao, et al., Sati and Gahalaut, 2013 that indicated that high intensity rainfalls, runoff and lake breaches frequently cause devastating floods. Even though, the slope in the central region of the state was less steep, it did not have much influence in the hazard map as it was awarded the lowest weight. Therefore, its overall contribution to causing hazard is just 5.5%, which is preceded by soil moisture index with 11.7% contribution. The values of maximum eigenvalue (λ_{maxH}) and CR, 4.1177 and 0.043 respectively, from equations (2) and (6) match the values from the analytical results of AHP. (see Table 5).

Flood Vulnerability Assessment:

Population, settlements and structures and road network are the most vulnerable to flood hazard. The population map is denser than the settlements, because the population map has considered the population at the tourist attractions as well. Millions of tourists visit many of the popular destinations, making some of the regions more populated than they are. According to table 5, 65% of the vulnerability factors is population, which is followed by 25% of settlements and structures. Only 10% of the total vulnerability factors is attributed to road network. The values of maximum eigenvalue (λ_{maxV}) and CR, 3.0381 and 0.032 respectively, from equations (8) and (12) closely match the values from the analytical results of AHP (see Table 6).

Flood Risk Assessment:

The higher flood risk regions are the areas that are not only highly populated, with larger settlements, more buildings and tourist attractions, but also receive high precipitation and have large number of drainage networks. These areas are also mostly valleys surrounded by steep mountains. The hydroelectric power plant locations map (Figure 13) was created using the data from NRSC's (National Remote Sensing Center of India) WRIS (Water Resources Information System of India) portal (WRIS NRSC). As seen in some of the literature, Hydroelectric power plants are now being considered as a potential cause for increasing the effects of flood, thereby increasing the hazard. From the power plant map (Figure 13), it is evident that most of these plants are situated in very high-risk regions.

The flood risk evaluation map (Figure 13) has historical flood events data overlaid on the risk map. The dot densities represented by small blue dots indicate small number of flood events, where as the large purple ones indicate large number of major flood events. From the map, it is evident that majority of the purple dots coincide with red high-risk regions. This shows that the method and the data sets used in this research produced verifiable results in relation to historically recorded flood events. These results could definitely be improved with better data, inputs and applying qualitative methods.

SUMMARY, CONCLUSION AND FUTURE WORK

Uttarakhand is a land of steep Himalayan mountains, dense perennial river networks, home to a host of pilgrim and tourist places, attracting thousands of people from across the world. The region is situated in a seismic active zone, and the recent urbanization has made the state more unstable. The state is also known for adverse weather conditions, which receives high intense rainfall and frequent cloudbursts. All these factors are responsible for the state being prone to flood disasters. Recent devastating flash floods have raised concerns regarding disaster management methods.

In this research, we identified regions highly prone to flood events and recognized precipitation and drainage networks as the main causes. Many historical flood events took place in the high-risk zones. Using the flood risk maps, several measures could be taken to improve the disaster management methods in the future. For instance, distance from the river networks could be considered to develop better strategies to protect the settlements in case of a disaster. Road network and drainage network maps could be used to plan evacuation routes. Anthropogenic factors like deforestation, constructions projects and hydro power plant projects have increased the frequency and intensity of floods. Power plant projects involve digging and blasting of vast land areas, and since Uttarakhand is in a seismically active zone, these activities make the region more unstable, and lead to multiple disasters like floods, landslides and mudslides. There is a lot of scope for further analysis in this regard. For instance, Geostatistical analysis could shed more light on the correlation between power plants and flood hazard. More comprehensive hydroelectric power plant data with geological and vegetation data could also be considered in the future works.

ACKNOWLEDGEMENT

Analyses and visualizations used in this paper were produced with the Giovanni online data system, developed and maintained by the NASA GES DISC. We acknowledge the TRMM mission scientists and NASA personnel for the production of data used in this research. SRTM 30m DEM data was retrieved from USGS Earth Explorer portal, courtesy of the NASA Land Processes Distributed Active Archive Center (LP DAAC), USGS Earth Resources Observation and Science (EROS) Center, Sioux Falls, South Dakota. Climate Prediction Center (CPC) Soil Moisture Data provided by National Oceanic and Atmospheric Administration's (NOAA) / OAR/ Earth System Research Laboratory (ESRL), Physical Science Division (PSD), Boulder, Colorado, was obtained from the website https://www.esrl.noaa.gov/psd/.

REFERENCES

Acker, J. G., Leptoukh, G. (2007) Online analysis Enhances Use of NASA Earth Science Data, *EOS, Transactions of the American Geophysical Union*, 88,2, 14 – 17 url: https://giovanni.gsfc.nasa.gov/giovanni/

Azmeri, Hadihardaja, Iwan K., Vaidya, Rika (2016) Identification of Flash Flood Hazard zones in mountainous small watershed of Aceh Besar Regency, Aceh Province, Indonesia, *The Egyptian Journal of Remote Sensing and Space Science*, 19, 1, 143 – 160, doi: 10.1016/j.ejrs.2015.11.001

Bhambri, Rakesh, Metha, Manish, Dobhal, D.P., Gupta, Anil Kumar, Pratap, Bhanu, Kesarwani, Kapil, Verma, Akshaya (2016) Devastation in the Kedarnath (Mandakini) Valley, Garhwal Himalaya, during 16 – 17 June 2013: A Remote Sensing and Ground-Based Assessment, *Nat Hazards*, 80, 3, 1801 - 1822, doi: 10.1007/S11069-015-2033-y.

Bhatt, Ganesh D., Sinha, Komal, Deka, P. K., Kumar, Ajay (2014) Flood Hazard and Risk Assessment in Chamoli District, Uttarakhand Using Satellite Remote Sensing and GIS Techniques, *International Journal of Innovative Research in Science, Engineering and Technology*, 3, 8, 15348 - 15356, doi: 10.15680/IJIRSET.2014.0308039.

Bonacci, O., Ljubenkov, I., Roje-Bonacci, T. (2006) Karst Flash Floods: An Example from the Dinaric Karst (Croatia), *Natural Hazards and Earth System Science*, 6, 2, 195-203

Cho, Changrae., Li, Rong., Wang, S. Y., Yoon, Jin-Ho, gillies, Robert R. (2016) Anthropogenic Footprint of Climate Change in the June 2013 Northern India Flood, *Climate Dynamics*, 46, 3, 797 - 805, doi: 10.1007/s00382-015-2613-2.

Danumah J. H., Odai, S. N., Saley, B. M. et al. (2016), *Geoenvironment Disasters*, 3: 10.

Dhar, O. N., Nandargi, Shobha (2003) Hydrometeorologiccal Aspects of Floods in India, Natural Hazards, 28, 1, 1 – 33, doi: 10.1023/A:1021199714487

Dobhal, D. P., gupta, A. K., Mehta, M., Khandelwal, D. D. (2013) Kedarnath Disaster: Facts and Plausible Cause, *Current Science*, 105, 171 – 174

Doocy, Shannon, Daniels, Amy, Murray, Sarah, Kirsch, Thomas D. (2013) The Human Impact of Floods: A Historical Review of Events 1980-2009 and Systematic Literature Review. *PLOS Currents Disasters*. Edition 1. doi: 10.1371/currents.dis.f4deb457904936b07c09daa98ee8171a.

Dool, Huug van den, Huang, Jin, Fan J., Yun (2003) Performance and Analysis of the Constructed Analogue Method Applied to US Soil Moisture Applied over 1981-2001, *Journal of Geophysical Research*, 108, 1 – 16.

Gilard, Olivier (2016) Hazard, Vulnerability and Risk in Climate Change and Agriculture Worldwide, Springer Netherlands, ISBN 978-94-017-7462-8, doi:10.1007/978-94-017-7462-8

Hill, Christopher D., Verjee, Firoz (2010) Flash Flood Science in Flash Flood Early Warning System Reference Guide, COMET, University Corporation for Atmospheric Research (UCAR), ISBN 978-0-615-37421-5, url: http://www/meted.ucar.edu/hazwarnsys/haz_fflood.php

Ismail Elkhrachy (December 2015), Flash Flood Hazard Mapping Using Satellite Images and GIS Tools: A Case Study of Najran City, Kingdom of Saudi Arabia (KSA), *The Egyptian Journal of Remote Sensing and Space Science*, Volume 18, Issue 2, Pages 261 – 278, ISSN 1110 – 9823

Kazakis, Nerantzis, Kougias, Ioannis, Patsialis, Thomas (December 2015) Assessment of Flood Hazard Areas at a Regional Scale Using an Index – Based Approach and Analytical Hierarchy Process: Application in Rhodope – Evros Region, Greece, *Science of The Total Environment*, 538, 555 – 563, doi: 10.1016/j.scitotenv.2015.08.055

Kobrick, Michael, Crippen, Robert, doi: 10.5067/MEaSUREs/SRTM/SRTMGL1.003

Mapcruzin: http://www.mapcruzin.com/free-india-country-city-place-gis-shapefiles.htm

Martha, Tapas R., Roy, Priyom, Govindharaj, K. Babu, Kumar, K. Vinod, Diwakar, P. G., Dadhwal, V. K. (2015) Landslides Triggered by the June 2013 Extreme Rainfall Event in Parts of Uttarakhand State, India, *Landslides*, 12, 1, 135 - 146.

Mateeul Haq, Memon Akthar, Sher Muhammad, Siddiqi Paras, Jillani Rahmatullah (December 2012), Techniques of Remote Sensing and GIS for Flood Monitoring and Damage Assessment: A Case Study of Sindh Province, Pakistan, *The Egyptian Journal of Remote Sensing and Space Science*, Volume 15, Issue 2, Pages 135 – 141, ISSN 111 – 9823

Matori, Abd Nasir, Lawal, Dano Umar, Yusof, Khamaruzaman Wan, Hashim, Mustafa Ahmad, Balogun, Abdul – Lateef (2014) Spatial Analytic Hierarchy Process Model for Flood Forecasting: An Integrated Approach, *IOP conference Series: Earth and Environment Science*, 20, 1, 012029, doi: 10.1088/1755-1315/20/1/012029

NASA LP DAAC, (2000) SRTMGL1: NASA Shuttle Radar Topography Mission Global 1 Arc Second Version 003, 31.469º N, 79.062º E, 30.25º N, 81.02º, 29.56o N, 77.99o E, 31.06o N, 77.806o E. NASA EOOSDIS

Land Processes DAAC, USGS Earth Resources Observation and Science (EROS) Center, Sioux Falls, South Dakota, https://lpdaac.usgs.gov, accessed April 2016 at https://earthexplorer.usgs.gov/

National Research Council (2005) Flash Floods in Flash Flood Forecasting Over Complex Terrain: With an Assessment of the Sulphur Mountain NEXARD in Southern California, The National Academics Press, 12 – 25, doi: 10.17226/11128

Ocampo Lopez O., Velez Upegui J (2014) The Use of Remote Sensing Data in a Colombian Andean Basin for Risk Analysis. In: Padro – Iguzquiza E., Guardiola – Albert C., Heredia J., Moreno – Merino L., Duran J., Vargas – Guzman J. (eds), *Mathematics of Planet Earth*. Lecture Notes in Earth System Sciences. Springer, Berlin, Heidelberg.

Pande, Ravindra K. (2010) Flash Flood Disasters in Uttarakhand, *Disaster Prevention and Management: An International Journal*, 19, 5, 565-570, doi: 10.1108/09653561011091896

Rao, Durga K.H.V., Rao, Venkateshwar V., Dadhwal, VK, Diwakar, P. G. (2014) Kedarnath Flash Floods: A Hydrological and Hydraulic Simulation Study, *Current Science*, 106, 4, 598 – 603.

Ray, P. K. Champati, Chattoraj, Shovan Lal, Bisht, M.P.S., Kannaujiya, Suresh, Pandey, Kamal, Goswami, Ajanta (2016) Kedarnath Disaster 2013: Causes and Consequences using Remote Sensing Inputs, *Natural Hazards*, 81, 227 - 243, doi: 10.1007/s11069-015-2076-0.

Saaty, Thomas L. (1990). How to Make a Decision: The Analytical Hierarchy Process, *European Journal of Operational Research*, 48, 1, 9 – 26, doi: 10.1016/0377-2217{90)90057-I

Sandrp Wordpress: https://sandrp.wordpress.com/2013/07/10/uttarakhand-existing-under-construction-and-proposed-hydropower-projects-how-do-they-add-to-the-disaster-potential-in-uttarakhand/

Sati, S. P., Gahalaut, V. K., (2013) The Fury of the Flash Floods in the North-West Himalayan Region: The Kedarnath Tragedy, Geomatics, Natural Hazards and Risks, 4, 3, 193 – 201, doi: 10.1080/19475705.2013.827135

Shreshta, Dhruba Pikha, Zinck, J Alfred (2001) Land Use Classification in Mountainous areas: Integration of Image Processing, Digital Elevation Data and Field Knowledge, *International Journal of Applied Earth Observation and Geoinformation*, 3, 1, 78 – 85, ISSN 0303 – 2434, doi: 10.1016/s0303-2434(01)85024-8.

Sinha, R., Bapalu, G.V., Singh, L. K. et al. (2008) *J Indian Soc Remote Sens*, 36: 335

Stefanidis, Stefanos, Stathis, Dimitrios, (2013) Assessment of Flood Hazard Based on Natural and Anthropogenic Factors Using Analytic Hierarchy Process (AHP), *Natural Hazards*, 68, 2, 569 - 585, doi: 10.1007/s11069-013-0639-5

Sturdevant-Rees, Paula, Smith, James A., Morrison, Julia, Baeck, Mary Lynn (2001) Tropical Storms and the Flood Hydrology of the Central Appalachians, *Water Resources Research*, 37,8, 2143 – 2168, doi:10.1029/2000WR900310

UNISDR https://www.unisdr.org/we/inform/publications/46796

Van Westen, C.J., (2016) National Scale Landslide Susceptibility Assessment for SVG. CHARIM Caribbean Handbook on Risk Information Management, World Bank GFDRR, ACP-EU Natural Disaster Risk Reduction Program. www.charim.net

Wake, Bronwyn, (2013) Flooding Costs, *Nature Climate Change*, Nature Publishing Group, 3, 9, 778, doi: 10.1038/nclimate1997.

WRIS–NRSC:

http://india-wris.nrsc.gov.in/wrpinfo/index.php?title=Dhauliganga_Hydroelectric_Project_JH00677